

A Simple and Reliable Method to Determine Mean Incident Light Flux Densities on Cylindrical Photoreactors and Photobioreactors from a Unique Fluence Rate Measurement

Jean-François Cornet, Jérémi Dauchet, Thomas Vourc'h, Carolina Arnau, David Garcia-Gragera, Francesc Gòdia, Fabrice Gros, Enrique Peiro

▶ **To cite this version:**

Jean-François Cornet, Jérémi Dauchet, Thomas Vourc'h, Carolina Arnau, David Garcia-Gragera, et al.. A Simple and Reliable Method to Determine Mean Incident Light Flux Densities on Cylindrical Photoreactors and Photobioreactors from a Unique Fluence Rate Measurement. Industrial and engineering chemistry research, 2023, 62 (12), pp.4875-4884. 10.1021/acs.iecr.2c04151 . hal-04082101

HAL Id: hal-04082101
https://hal.science/hal-04082101

Submitted on 26 Apr 2023

HAL is a multi-disciplinary open access archive for the deposit and dissemination of scientific research documents, whether they are published or not. The documents may come from teaching and research institutions in France or abroad, or from public or private research centers.

L'archive ouverte pluridisciplinaire **HAL**, est destinée au dépôt et à la diffusion de documents scientifiques de niveau recherche, publiés ou non, émanant des établissements d'enseignement et de recherche français ou étrangers, des laboratoires publics ou privés.

A simple and reliable method to determine mean incident light flux densities on cylindrical photoreactors and photobioreactors from a unique fluence rate measurement

Jean-François Cornet[1], Jérémi Dauchet[1], Thomas Vourc'h[1(*)], Carolina Arnau[2], David Garcia-Gragera[2], Francesc Gòdia[2], Fabrice Gros[1], Enrique Peiro[2]

[1] Université Clermont Auvergne, Clermont Auvergne INP, CNRS, Institut Pascal, F-63000 Clermont-Ferrand, France.

[2] MELISSA Pilot Plant – Claude Chipaux laboratory, Universitat Autonoma de Barcelona, Bellaterra, Barcelona, 08193 Spain.

Corresponding Author

* Thomas VOURC'H

thomas.vourc-h@sigma-clermont.fr

ABSTRACT

A new method to determine the hemispherical incident light (photon) flux density onto cylindrical photoreactors or photobioreactors is presented. It applies for situations where the photo(bio)reactor is radially illuminated by surrounding artificial sources or solar light. It relies on the direct measurement of a fluence rate with a spherical sensor put at the center of the reactor. Theoretical relations leading to the calculation of the hemispherical incident light flux density from the fluence rate value are established, and a web application performing those calculations is made available. It relies on a view factor, the expression of which, established for the first time with any assumption of the angular distribution of light at the boundary, is given. This requires to define properly the degree of collimation for the incident radiation field. Two different and complementary experimental devices are used to validate the method. As a result, the proposed method appears to be simple and reliable; it even looks faster and more accurate than actinometry for this particular geometry.

INTRODUCTION

The use of solar or artificially-illuminated photoreactors and photobioreactors (P(B)R) is increasing with the growing interest in photo-reactive processes. They are used for the development of microalgae with various applications [1], the depollution of liquid [2-4] and gaseous effluents [5-6], the production of solar fuels [7-8], the synthesis of molecules of interest for chemistry and fine chemistry [9], the synthesis of platform molecules and high-value products, etc. Different geometries co-exist [10-11], but for many processes, the cylindrical geometry predominates as it presents a large specific illuminated area and is suitable for controlling reactor mixing. Regardless of geometry, radiative transfer always controls the kinetic and energetic performances of a P(B)R [12] and the first quantity that determines the maximum performances of a P(B)R is the mean hemispherical incident light flux density on the illuminated surface. This is the reason why it is of considerable importance to know accurately its value [12-14]. Several methods exist for this, each with their strengths and weaknesses.

Mapping from a flat hemispherical incident flux density sensor is often used because it is quite easy to implement, but suffers from a significant lack of accuracy because it is difficult to take into account the heterogeneities often existing at the level of light sources or to be adapted to cylindrical geometries [15].

Actinometry may be preferred; it perfectly averages the surface heterogeneities, but appears much more tedious to implement, especially in cylindrical or complex geometries [14, 16-17].

Many cylindrical P(B)R are radially illuminated with a surrounding light source device, since this design is more favorable in terms of specific illuminated area compared to an annular reactor with a central light source. They can be either artificially-illuminated reactors or solar reactors with cylindrical parabolic compounds. In this particular case, there is another method based on the central measurement of fluence rate with a spherical sensor. This method is very simple to implement and can be extremely accurate if the theory for deducing the average hemispherical incident light flux density is properly established. The purpose of this article is to present in detail this accurate, simple and reliable method with the help of all the necessary theoretical developments. The proposed approach will then be confronted with experimental results to validate the method in two different and complementary situations, using different lamps, angular distributions of incident radiation as well as different geometries and scale factors.

MATERIALS AND METHODS

This section presents the two experimental devices of photo(bio)reactors used in this article to validate the methodology together with important considerations regarding fluence rate measurement and conversion units.

Lighting system and measurements for the photo(bio)reactor with halogen lamps BAB 36-38°

The first experimental device used in this study is a photo(bio)reactor illuminated by halogen lamps. In more details, the lighting system is composed of 55 halogen lamps BAB 36-38° radially arranged with a **fixed** internal radius for emission R_C = 12 cm. The internal radius of

the P(B)R is $R_{P(B)R}$ = 8 cm and the semi-height of the vessel is H = L/2 = 14 cm (see Figure 1). The working volume of this reactor is 5 L.

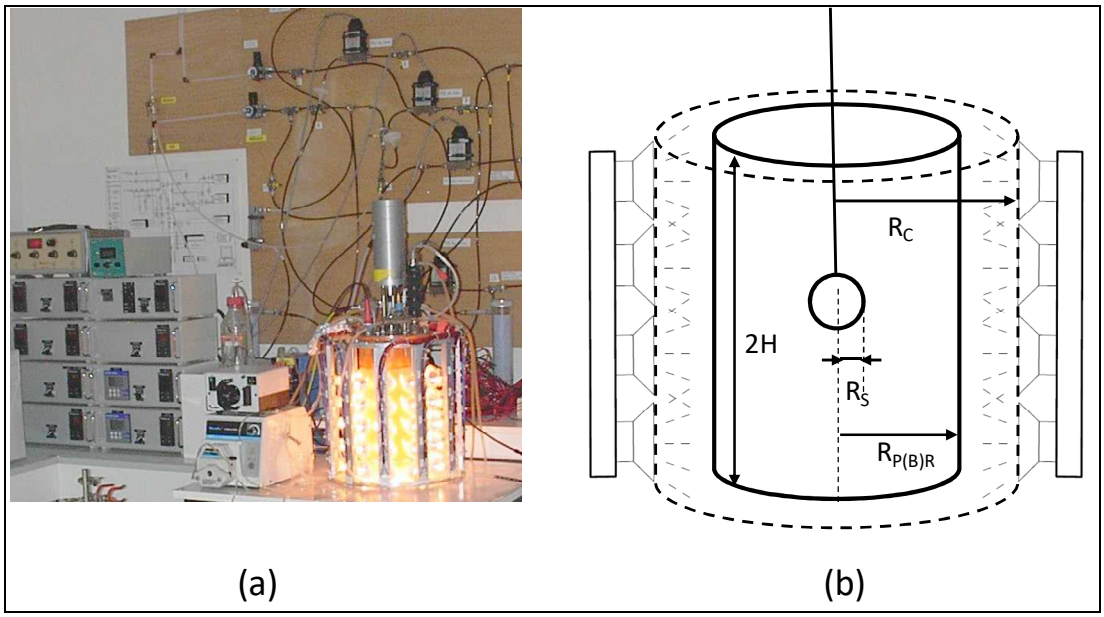


Figure 1: Representation of the P(B)R with the illuminating device using 55 BAB 36-38° halogen lamps. (a) Photograph of the P(B)R and (b) Scheme for the main variables and sensor location under experimental fluence rate measurement procedure.

For a beam angle of 36-38° given by the manufacturer for this kind of lamps (Osram, Sylvania,....), *i.e.* a viewing angle of 18.5°, equation (16) gives the degree of collimation n = 13 (see Figure 2 and theoretical section).

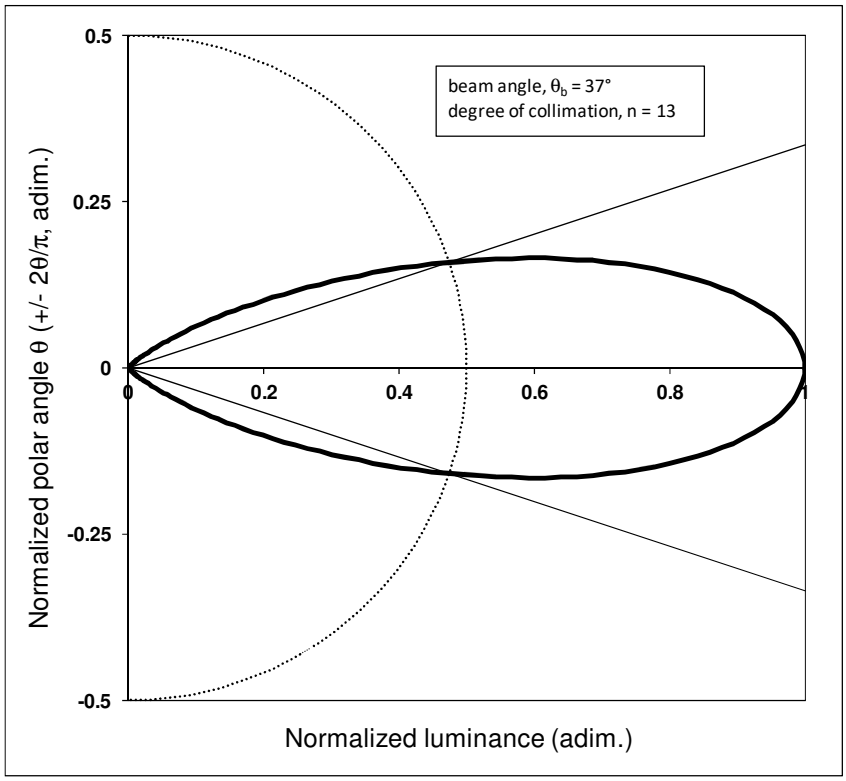


Figure 2: Polar representation of the normalized luminance ($L(\theta)/L_{max}(0)$, thick line) with a degree of collimation ***n* = 13**. Case of halogen lamps BAB 36-38° with a mean beam angle of 37° (thin line). The dotted line represents the location of iso-luminances independent of the θ angle for half of the maximum normalized luminance value ($L(\theta)/L_{max}$ = ½), corresponding to the definition of the beam angle.

In this case, we have performed the measurement of photon fluence rates with two sensors of **different diameters**: a Li-COR (LI-193SA) sensor with a radius R_S = 3 cm (the same as for the second case study hereafter depicted) and a Waltz milli-sensor (US-SQS-I, commercialized by Li-COR) with a radius R_S = 0.15 cm. For these two sensors, we have calculated the view factor $F_{C\rightarrow S}$ according to Eqs. (20) and (23) hereafter with the Monte Carlo algorithm (see Supporting Information). The results are summarized in Table 1, in the Results & Discussion section of the paper.

Lighting system and measurements for the photo(bio)reactor with LEDs + optics

For this second experimental device, the lighting system is composed of 80 white LEDs + optics by panel × 8 panels arranged in two octagonal identical layouts around the two cylindrical parts of the reactor (for a total of 640 LEDs). The radius of the P(B)R is $R_{P(B)R}$ = 7.5 cm and the semi-height of the vessel is H = L/2 = 75 cm (see Figure 3). The working volume of this reactor is roughly 85 L.

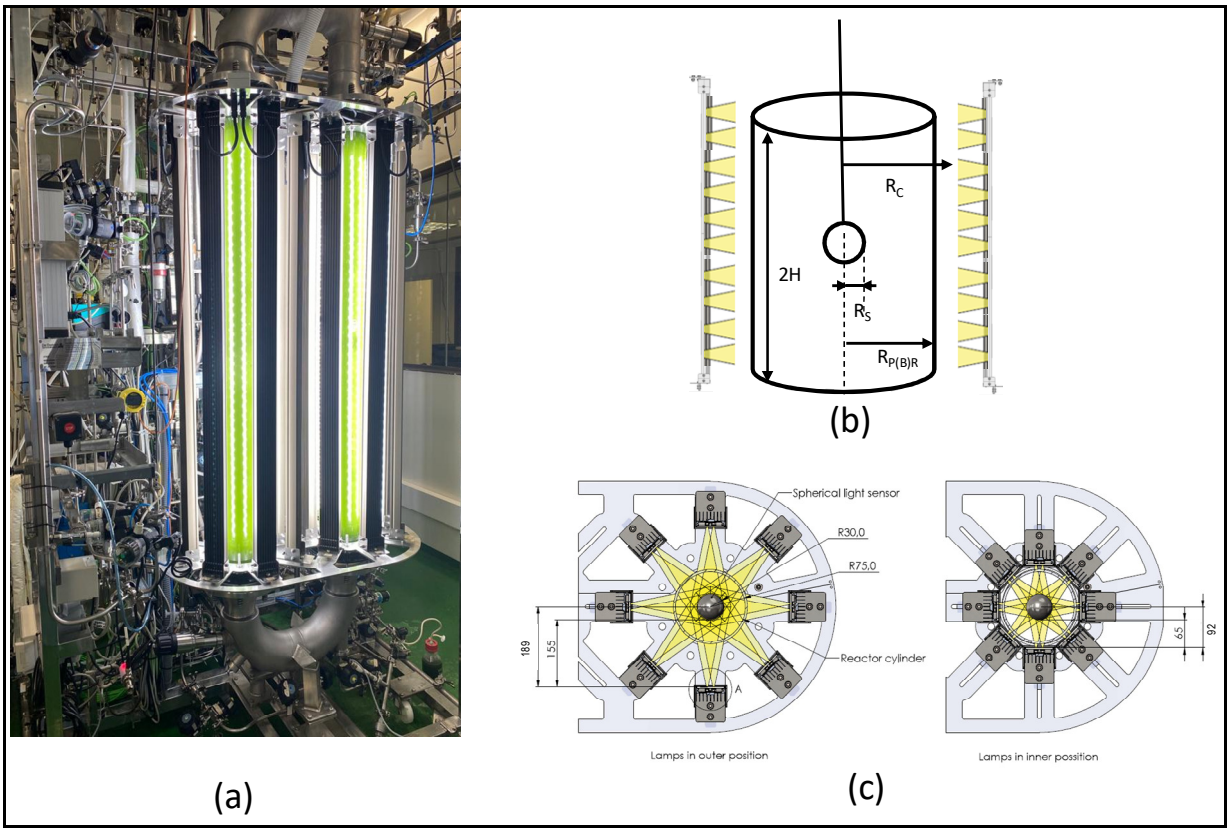


Figure 3: Representation of the P(B)R with the illuminating device composed of 80 white LEDs + optics by panel × 8 panels arranged in two octagonal identical layouts around the two cylindrical parts of the reactor. In this case, the beam angle is of 24°. (a) Photograph of the P(B)R, (b) Scheme for the main variables and sensor location under experimental fluence rate measurement procedure and (c) Top view for different measurement positions of the sources at distance R_C during fluence rate (ψ) measurement (distance units are in mm).

For a beam angle of 24° given by the manufacturer of the LEDs (Luxeon, Sunplus 20), *i.e.* a viewing angle of 12°, equation (16) gives the degree of collimation n = 31 (see Figure 4 and theoretical section).

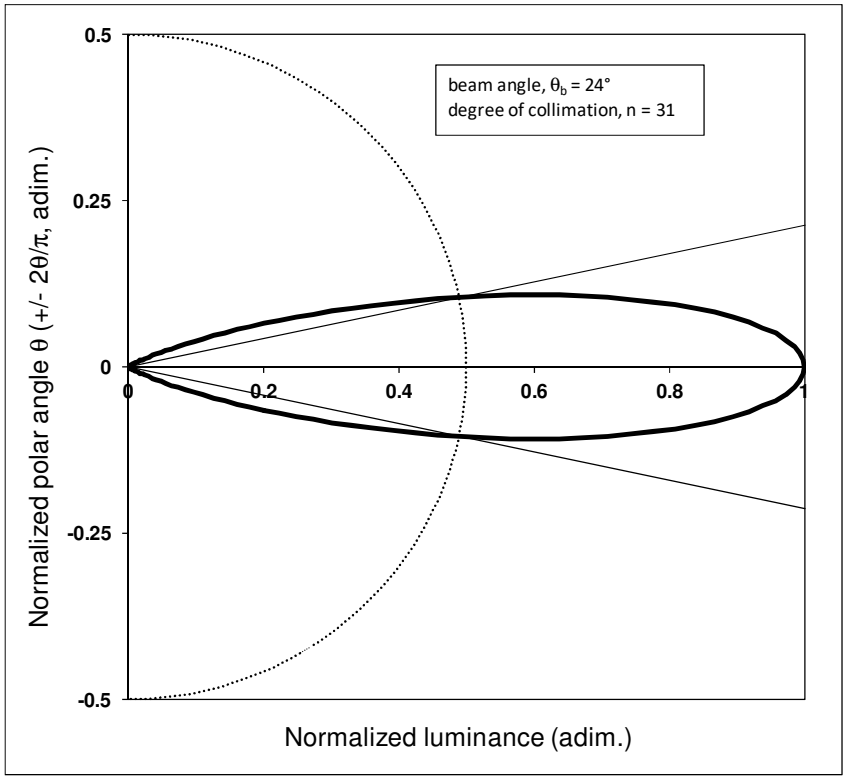


Figure 4: Polar representation of the normalized luminance ($L(\theta)/L_{max}(0)$, thick line) with a degree of collimation ***n* = 31**. Case for white LEDs + optics with a mean beam angle of 24° (thin line). The dotted line represents the location of iso-luminances independent of the θ angle for half of the maximum normalized luminance value ($L(\theta)/L_{max}$ = ½), corresponding to the definition of the beam angle.

Measurement of photon fluence rates with a Li-COR (LI-193SA) sensor (**fixed** radius R_S = 3 cm) have been performed with three lamps positions with **varying** emission distance R_C =

9.2 cm – 13.9 cm – 18.9 cm. For these three situations, we have calculated the view factor $F_{C\rightarrow S}$ according to Eqs. (20) and (23) hereafter with our Monte Carlo algorithm (see Supporting Information). The results are summarized in Table 2, in the Results & Discussion section of the paper.

Fluence rate measurement

It is very important here to point out that, whatever the external lighting device used as emitting source and its surface heterogeneity, the measurement of the fluence rate by a spherical sensor placed in the center of a cylindrical tank and which is moved from bottom to top has a remarkable stability. The measurement obtained is very accurate (better than +/- 5%) and perfectly averages the fluctuations observed at the emitting wall, even with the very small diameter sensor (3 mm). The two sensors used are quantum-meters delivering the fluence rate in $\mu mol_{h\nu}.m^{-2}.s^{-1}$ in the visible light spectrum (more precisely in the photosynthetically active radiation PAR [400 – 700 nm]), but the results for incident radiant flux densities q_R are given hereafter in $W.m^{-2}$ (in the same range of wavelengths). The conversion factors for each kind of illuminating source have been obtained by the following relation from the knowledge of the lamp energy distribution spectrum E_λ (pdf) given by the suppliers [18]:

$$1\ W.m^{-2} = \frac{\int_{400\ nm}^{700\ nm} E_\lambda \lambda\ d\lambda}{1.1974 \times 10^{-7} \int_{400\ nm}^{700\ nm} E_\lambda d\lambda}\ \mu mol_{h\nu}.m^{-2}.s^{-1} = \frac{\lambda_{m,w}}{1.1974 \times 10^{-7}}\ \mu mol_{h\nu}.m^{-2}.s^{-1}$$

where the term 1.1974×10^{-7} is obtained from the Avogadro number, the Planck constant h and the light celerity in vacuum c_0 from: $1.1974 \times 10^{-7} = 6.02 \times 10^{17} \times h \times c_0$.

This leads to the following conversion factors in the PAR range of wavelengths:

- for the white halogen lamps BAB: 1 $W.m^{-2}$ = 5.1 $\mu mol_{h\nu}.m^{-2}.s^{-1}$

- for the white LEDs used: 1 $W.m^{-2}$ = 4.6 $\mu mol_{h\nu}.m^{-2}.s^{-1}$

THEORETICAL CONSIDERATIONS

The aim of this theoretical section is to establish rigorously the relations between the fluence rate measurement ψ by a spherical sensor (radius R_S) located at the centre of a cylindrical and radially illuminated device (cylinder of radius R_C, see Figure 5) and the hemispherical mean incident photon (or radiative) flux density q_0 (PFD) at the wall of this device. By "mean" it is assumed here that this incident PFD is homogeneous on the emitting surface; even if practically it is not the case (it is generally not the case), we will observe in the experimental result section that this assumption gives excellent (accurate) results with much less effort than using actinometry for example. In this work, we will also assume a cosine power law for the angular distribution of the emission directions; this law allows to describe a full range of situations from collimated to Lambertian sources.

Once the hemispherical flux density at the emitting wall q_0 is known, it is then easy, using the conservation law for radiant energy, to calculate the incident PFD at any concentric cylindrical wall located inside the emitting cylinder (with a radius $R_{P(B)R}$), *i.e.* the incident PFD q_R for any photo(bio)reactor. In such conditions, this incident PFD q_R corresponds to the radiative source at the boundary (rear of the vessel wall). This PFD along with q_R homogeneity assumption and cosine power law for emission directions fully provide the boundary condition for the

photoreactive process. The general system of coordinates, the main considered variables and the angular distribution of light at the boundaries are summarized on Figure 5.

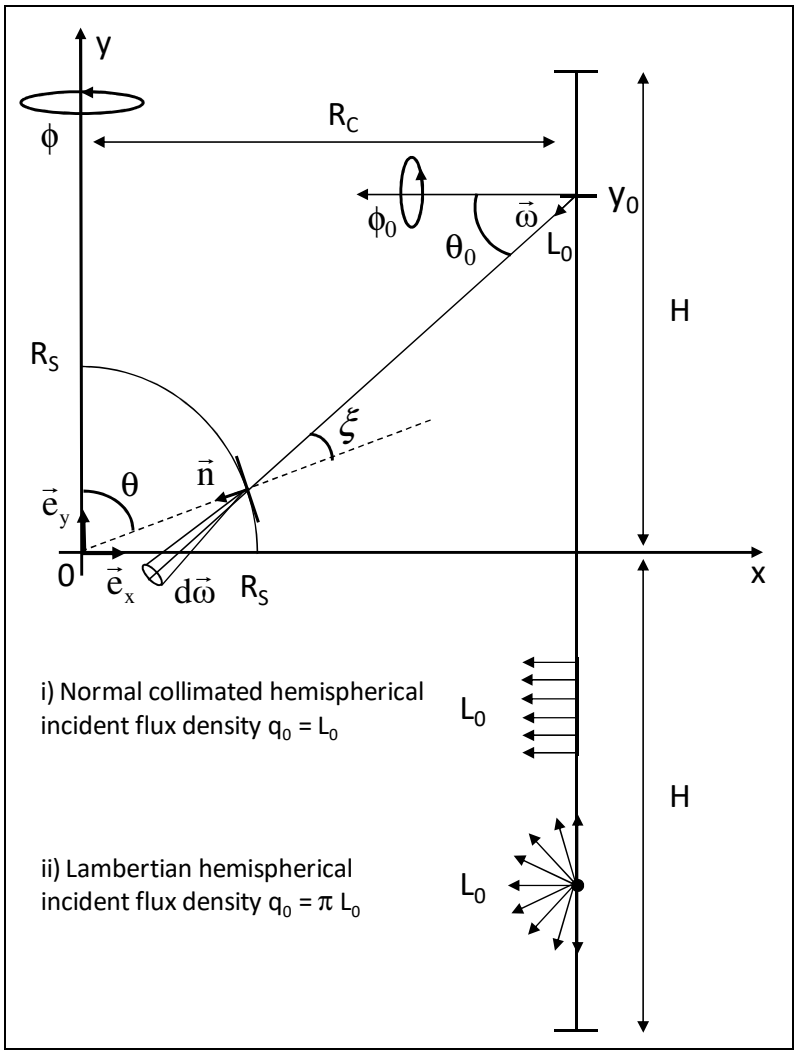


Figure 5: Notations for the academic case establishing relations between the fluence rate ψ (measured by a spherical sensor of radius R_S at the centre of an illuminating cylindrical device of radius R_C and height L = 2H) and the radial hemispherical incident photon flux density q_0 (at the sources) for i) a normal collimated incidence, and ii) a Lambertian (diffuse) incidence.

Definition of the fluence rate ψ measured by the spherical sensor

Any spherical sensor is calibrated to measure a photon (or radiant) fluence rate defined by the double integral [18-19]:

$$\psi = \frac{\iint_S d\vec{r}\, \vec{q}_{\cap}(\vec{r}) \cdot \vec{n}(\vec{r})}{\pi R_S^2} = \frac{1}{\pi R_S^2} \iint_S d\vec{r} \int_{2\pi^+} d\vec{\omega}\, L(\vec{r},\vec{\omega})\, \vec{\omega} \cdot \vec{n}(\vec{r}) = \frac{1}{\pi R_S^2} \iint_S d\vec{r} \int_{2\pi^+} d\vec{\omega}\, L(\vec{r},\vec{\omega}) \cos\xi \quad (1)$$

in which the directional quantity $L(\vec{r},\vec{\omega})$ is the luminance. The luminance is also referred in textbooks of radiative heat transfer as specific intensity (*I*) [20]. This definition ensures that for $R_S \rightarrow 0$, ψ tends to the spherical irradiance $G(\vec{r}) = \iint_{4\pi} L(\vec{r},\vec{\omega})\, d\vec{\omega}$ [18-19]. Alternatively, Eq. (1) may be also rewritten in a simple way from the total radiative flux received by the sensor Q_S:

$$\psi = \frac{Q_S}{\pi R_S^2} \quad (2)$$

Relations for the total radiative flux Q_S at the sensor surface

In this context, the establishment of a relation between the measured fluence rate ψ and the unknown hemispherical incident flux density q_0 becomes then a ”simple” problem of radiation exchange between surfaces. This approach is extremely well documented in the literature [20] and requires knowing the radiative view factor of the given studied geometry:

- $F_{S\to C}$ is the view factor of the sensor (S) toward the surrounding cylinder (C);

- $F_{C\to S}$ is the view factor of the surrounding cylinder (C) toward the sensor (S).

The radiative balance in the system is then straightforward (since the surrounding cylinder of radius R_C and height 2H is the unique radiative source):

$$Q_{C\to S} = Q_C\, F_{C\to S} = q_0\, 2\pi R_C\, 2H\, F_{C\to S} = Q_S \quad (3)$$

Using Eq. (2-3), we then obtain the following useful relationship:

$$\psi = \frac{Q_S}{\pi R_S^2} = \frac{Q_C\, F_{C\to S}}{\pi R_S^2} = \frac{q_0\, 4R_C H}{R_S^2} F_{C\to S} \quad (4)$$

This equation demonstrates that it is possible to find the relation between the fluence rate ψ and the incident PFD q_0 (at the sources) from the knowledge of only the view factor $F_{C\to S}$. Moreover, once q_0 is known, it will be easy to determine the incident PFD q_R on any concentric cylindrical surface with same height (the reactor vessel surface $A_{P(B)R}$) located between the sources and the spherical sensor of fluence rate ($R_S < R_{P(B)R} < R_C$, see Figures 1 & 3) by applying the conservation of the radial radiative flux Q_r:

$$Q_r = \text{cte} = q_0\, 2\pi R_C\, 2H = q_R\, 2\pi R_{P(B)R} L_{P(B)R} \quad (5)$$

i.e., since $2H \simeq L_{PBR}$:

$$q_R = q_0 \frac{R_C}{R_{P(B)R}} \quad (6)$$

The practical relations if the incident luminance (intensity) is isotropic in any direction $\vec{\omega}$ (Lambertian boundary condition) from classical approach of radiative thermodynamic equilibrium (black body theory)

In this case, at the boundary of the cylinder (the source), the incident luminance (intensity) is independent of the direction $\vec{\omega}$ and has the same value L_0 in any incoming direction (see Figure 5). Consequently, the hemispherical incident flux density (the unknown of the problem) is given by (see Figure 5): $q_0 = \pi L_0$. Additionally, this situation is described in the literature providing the view factor $F_{S\to C}$ [21] and using the reciprocity relation that is available in the case of equilibrium – Lambertian – boundary conditions

$$A_C F_{C\to S} = A_S F_{S\to C} = 2\pi R_C 2H F_{C\to S} = 4\pi R_S^2 F_{S\to C} \quad (7)$$

we obtain the view factor $F_{C\to S}$:

$$F_{C\to S} = \frac{R_S^2}{R_C H\sqrt{1+\left(\frac{R_C}{H}\right)^2}} = \frac{R_S^2}{R_C\sqrt{H^2+R_C^2}} \quad (8)$$

Finally, substituting this equation into the general expression (4) gives the expression of the incident PFD:

$$q_0 = \frac{\psi \sqrt{1+\left(\frac{R_C}{H}\right)^2}}{4} \qquad (9)$$

Attention must be paid here, however, to the fact that this definition imposes to put the spherical sensor at the middle of the total height L = 2H (see Figure 5) of the cylinder [21].

The practical relations if the incident luminance is perfectly collimated (with normal incidence)

In this case, at the boundary of the cylinder, the incident luminance (intensity) is non-zero only in the direction $\vec{\omega} = -\vec{e}_x$ and takes the form $L(\vec{r},\vec{\omega}) = L_0 \delta\left(\vec{\omega} - \vec{e}_x\right)$ where $\delta(x\text{-}a)$ is the Dirac distribution centred in a. The view factor of the problem is not published in the literature, but in this simple situation, we can envisage to evaluate directly the fluence rate from its integral formula (Eq. 1). In cylindrical coordinates indeed, as already mentioned, we must verify the radial radiative flux conservation (Q_r = cte), *i.e.* a concentration effect in the form: $L(r) = q_0 \frac{R_C}{r}$. Especially, for the integration on the fluence rate sensor area, and restricting the application conditions to H > R_S (see Figure 5), we have ($dQ_C = q_0 R_C dz\, d\phi = dQ_S = L_0 R_S dz \sin\theta\, d\phi$):

$$L_0(r) = q_0 \frac{R_C}{R_S \sin\theta} \qquad (10)$$

The definition of the fluence rate (Eq. 1) may then be rewritten as follows:

$$\psi = \frac{1}{\pi R_S^2} \int_0^{2\pi} d\phi \int_0^{\pi} d\theta \sin\theta R_S^2 L_0(r) \left(-\vec{e}_x \cdot \vec{n}(\theta)\right) \quad (11)$$

Because the normal $\vec{n}(\theta)$ is clearly a function of the angle θ in the integration (see Figure 5) with the components:

$$\vec{n}(\theta) = \begin{vmatrix} -\sin\theta \\ -\cos\theta \end{vmatrix}$$

we have $-\vec{e}_x \cdot \vec{n}(\theta) = \sin\theta$ and then from Eqs. (10) and (11):

$$\psi = \frac{2\pi R_S^2}{\pi R_S^2} q_0 \frac{R_C}{R_S} \int_0^{\pi} d\theta \sin\theta = 2q_0 \frac{R_C}{R_S} \left[-\cos\theta\right]\Big|_0^{\pi} = 4q_0 \frac{R_C}{R_S} \quad (12)$$

Finally, Eq. (12) leads to the practical relationship giving the hemispherical incident quasi-collimated flux density q_0 from the experimental measurement of the fluence rate ψ from:

$$q_0 = \frac{\psi R_S}{4R_C} \quad (13)$$

It must be noticed that using Eq. (4) with Eq. (12) enables to demonstrate that the view factor is:

$$\begin{aligned} F_{C\to S} &= \frac{R_S}{H} \quad \text{if } H > R_S \\ F_{C\to S} &= 1 \quad \text{if } H < R_S \end{aligned} \quad (14)$$

which is of course, a very intuitive value for a normal collimated incidence (see Figure 5).

The practical relations if the incident luminance is neither collimated nor Lambertian but diffuse with any degree of collimation $0 < n < \infty$ – The general case.

In this general situation, any point source of light emits a radiation in a cone of beam angle θ_B (twice the viewing angle θ_v) with azimuth symmetry over $\phi = 2\pi$. This situation is here approached by a directional distribution of the luminance $L_0(\vec{\Omega})$ assumed to obey the cosine power law:

$$L_0(\theta_0, \phi_0) = L_0 \cos^n(\theta_0) \quad (15)$$

where *n* is called the degree of collimation of the radiation field (a real value, not necessarily an integer). This law is often used to simply model the radiation pattern of sources [22] as the simplest one, among more complicated approaches [23].

From this definition, any radiation field may be represented if θ_v (or beam angle θ_B) is known and *n* determined in agreement with this information generally given by the manufacturer. For this, one needs to identify the correct value of *n* fitting with the definition of the viewing angle (see above Figures 2 & 4) for which the luminance is 50% of the direct forward luminance ($\theta = 0$), *i.e.*:

$$\cos^n(\theta_V) = ½ \text{ or } n = \frac{\ln(\frac{1}{2})}{\ln(\cos\theta_V)} \quad (16)$$

Eq. (15) then enables to treat any incident characteristic of the source between the collimated case ($n = \infty$) and the Lambertian case ($n = 0$) discussed above.

In this general case, the incident flux density at the source is always given from Eq. (4) by:

$$q_0 = \frac{\psi R_S^2}{4 R_C H \, \mathrm{F}_{\mathrm{C}\to\mathrm{S}}} \quad (17)$$

and the incident flux density at the rear PBR wall from Eq. (6):

$$q_R = \frac{\psi R_S^2}{4 R_{P(B)R} H \, \mathrm{F}_{\mathrm{C}\to\mathrm{S}}} \quad (18)$$

In the two simple cases already discussed, the view factor $\mathrm{F}_{\mathrm{C}\to\mathrm{S}}$ has an analytical form:

- For diffuse – Lambertian incident luminance, n = 0 and the view factor is given by eq. (8), $\mathrm{F}_{\mathrm{C}\to S} = \dfrac{R_S^2}{R_C H \sqrt{1+\left(\dfrac{R_C}{H}\right)^2}}$
- For collimated incident luminance, $n = \infty$, and the view factor is given by eq. (14), $\mathrm{F}_{\mathrm{C}\to\mathrm{S}} = \dfrac{R_S}{H}$.

But for any other value of $0 < n < \infty$ generally encountered, the view factor $\mathrm{F}_{\mathrm{C}\to\mathrm{S}}$ must be defined and evaluated by a numerical procedure. The general definition of the view factor $\mathrm{F}_{\mathrm{C}\to\mathrm{S}}$ is given by:

$$\begin{aligned} \mathrm{F}_{\mathrm{C}\to S} &= \int_C d\vec{C}_0 \frac{1}{A_C} \int d\vec{\omega} \frac{L_0(\vec{C}_0, \vec{\omega})}{q_0} \cos\theta_0 \, \mathcal{H}\left(\Delta(\vec{C}_0; \vec{\omega}; R_S)\right) \\ &= \int_{-H}^{H} \frac{dy}{2H} \int_0^{2\pi} \frac{d\phi}{2\pi} \int_0^{2\pi} \frac{d\phi_0}{2\pi} \int_0^{\frac{\pi}{2}} d\theta_0 \cos^{n+1}\theta_0 \sin\theta_0 (n+2) \, \mathcal{H}(\Delta) \end{aligned} \quad (19)$$

where the incident photon flux density $q_0 = \int_{2\pi^+} d\vec{\omega} L_0(\vec{C}_0, \vec{\omega}) \cos\theta_0 = L_0 \frac{2\pi}{n+2}$ (according to eq. 15); A_C is the cylinder C area and $\mathcal{H}(\Delta)$ is the Heaviside generalized function which is 0 if Δ is negative and 1 if Δ is positive. Δ is a discriminant defining the condition that the half-line $\vec{C}_0 + \sigma\vec{\omega},\ \sigma \in [0;+\infty]$ starting from $\vec{C}_0 \in C$ in direction $\vec{\omega}$ at the cylinder boundary intercepts the spherical sensor. Because of the symmetry around the y axis, the integral on ϕ vanishes and introducing the notation μ = cos(θ), Eq. (19) becomes:

$$\mathrm{F}_{C\to S} = \int_{-H}^{H} \frac{dy}{2H} \int_{0}^{2\pi} \frac{d\phi_0}{2\pi} \int_{0}^{1} d\mu_0\, \mu_0^{n+1} (n+2)\, \mathcal{H}(\Delta) \quad (20)$$

From the notations defined on Figure 5 and the symmetry already discussed, we can easily define the $(\vec{e}_x, \vec{e}_y, \vec{e}_z)$ coordinates for the starting point vector $\vec{C}_0 = \begin{vmatrix} R_C \\ y \\ 0 \end{vmatrix}$ and the direction vector $\vec{\omega} = \begin{vmatrix} -\cos\theta_0 \\ \sin\theta_0 \cos\phi_0 \\ \sin\theta_0 \sin\phi_0 \end{vmatrix}$. The intersection with the spherical sensor $\vec{C}_0 + \sigma\vec{\omega} \in S$ leads to the following system:

$$\begin{aligned} R_C - \sigma\cos\theta_0 &= R_S \sin\theta\cos\phi \quad (a) \\ y + \sigma\sin\theta_0\cos\phi_0 &= R_S\cos\theta \quad (b) \\ \sigma\sin\theta_0\sin\phi_0 &= R_S\sin\theta\sin\phi \quad (c) \end{aligned} \quad (21)$$

Note that for convenience in this demonstration, because of a symmetry around the x axis, we have used y < 0 in order to have $\theta_0 \in \left[0;\frac{\pi}{2}\right]$. Taking the square of each term and summing, we get:

$$\left(R_C - \sigma\cos\theta_0\right)^2 + \left(y + \sigma\sin\theta_0\cos\phi_0\right)^2 + \left(\sigma\sin\theta_0\sin\phi_0\right)^2 = R_S^2 \quad (22)$$

Rearranging the polynomial finally leads to:

$$\sigma^2 + 2\left(y\sin\theta_0\cos\phi_0 - R_C\cos\theta_0\right)\sigma + R_C^2 + y^2 - R_S^2 = 0$$

the discriminant of which being:

$$\Delta = 4\left(y\sin\theta_0\cos\phi_0 - R_C\cos\theta_0\right)^2 - 4\left(R_C^2 + y^2 - R_S^2\right) \quad (23)$$

The sign of this discriminant concludes the demonstration since it allows to evaluate the Heaviside function $\mathcal{H}(\Delta)$ in Eq. (20) according to whether it is positive or negative. The view factor $F_{C\to S}$ given by the triple integral Eq. (20) can be easily interpreted as an expectation in the statistical point of view and evaluated by a numerical procedure using a Monte Carlo algorithm and a Python code summarized in Supporting Information. It enables to achieve the calculation of the view factor $F_{C\to S}$ for any degree of collimation *n* by solving Eqs (20) and (23) with a 95% confidence interval. A web application where the interested reader can implement this calculation is also made available at http://gspr.ip.uca.fr/fluence_rate_view_factor.

As already mentioned in the Materials & Methods section, two actual situations are presented in this article to illustrate the procedure in the general case:

a)- validation of the approach with a 5 L cylindrical photoreactor using white halogen lamps BAB 36-38° at constant R_C, but with two diameters of fluence rate sensors R_S;

b)- validation of the approach on a 85 L cylindrical photobioreactor using a scalable illuminating system with white LEDs 24° with a constant radius of sensor R_S but with three radii R_C for the distance of the sources.

Hence, for these two kinds of P(B)R, the view factor $F_{C\to S}$ has been evaluated by the Monte Carlo algorithm (see Supporting Information) from Eqs. (20) and (23) after specifying the degree of collimation *n* and the geometry for each case (radius sensor R_S, radius for the illuminating device R_C, radius for the P(B)R, $R_{P(B)R}$ and total height 2H).

Correction of interfaces from geometrical optics.

Experimentally and theoretically speaking, the final quantity that we try to evaluate q_R is the hemispherical incident photon flux density at the rear of the wall (glass, quartz, etc.) of the photo(bio)reactor (input of the reaction medium) in the case of radial illumination. If the fluence rate measurement is performed with the photo(bio)reactor filled with water or any solvent (using underwater sensors), so no correction is necessary in the incident PFD calculation q_R by the preceding relations (Eq. 18 for instance). At the opposite, if the fluence rate measurement is performed with an empty P(B)R (in air) or without P(B)R, it is possible to increase the accuracy of the q_R calibration from the knowledge of the reflectivity ρ of an air-material (glass) interface

correction. In case of a measurement in air (no vessel between the fluence rate sensor and the illuminating device), the calculated value of q_R must be finally roughly multiplied by a factor (1 – ρ) to take into consideration the air-glass interface (the second interface with water or any liquid has a negligible reflectivity). If the measurement is done with an empty cylindrical vessel (the photo(bio)reactor), then, the calculated value of q_R must be divided by (1 – ρ) because using finally aqueous solution inside the reactor (or any other solvent) almost completely extinguishes the reflectivity at that second interface.

In the general case (*i.e.* for any degree of collimation considering the incident radiation at the wall), the directional reflectivity $\rho(\theta)$ at an interface is a function of the angular direction θ and can be obtained, for unpolarized radiation, by the algebraic average, knowing the relative refractive index n_r between the glass and the fluid (air, water, etc.) [20]:

$$\rho_{\parallel}(\theta) = \left\{\frac{n_r^2\cos(\theta) - \sqrt{n_r^2 - \sin^2(\theta)}}{n_r^2\cos(\theta) + \sqrt{n_r^2 - \sin^2(\theta)}}\right\}^2$$

$$\rho_{\perp}(\theta) = \left\{\frac{\sqrt{n_r^2 - \sin^2(\theta)} - \cos(\theta)}{\sqrt{n_r^2 - \sin^2(\theta)} + \cos(\theta)}\right\}^2$$

$$\rho(\theta) = \frac{\rho_{\parallel}(\theta)+\rho_{\perp}(\theta)}{2} \quad (24)$$

The mean normalized reflectivity ρ is then obtained by the following integrals for any degree of collimation n:

$$\rho = \frac{2\pi L_0 \int_0^{\frac{\pi}{2}} \rho(\theta)\cos^n(\theta)\cos(\theta)\sin(\theta)\,d\theta}{2\pi L_0 \int_0^{\frac{\pi}{2}} \cos^{n+1}(\theta)\sin(\theta)\,d\theta} = \int_0^{\frac{\pi}{2}} \rho(\theta)\cos^{n+1}(\theta)(\mathrm{n}+2)\sin(\theta)\,d\theta$$

(25)

It is well known that for the two extreme situations (collimated and Lambertian incidence) already discussed, the integral (Eq. 25) is analytical [20]:

- Normal collimated radiation field ($n = \infty$): $\rho = \left(\frac{n_r-1}{n_r+1}\right)^2$

- Lambertian radiation field (n = 0):

$$\rho = \frac{1}{2} + \frac{(3n_r+1)(n_r-1)}{6(n_r+1)^2} + \frac{n_r^2(n_r^2-1)^2}{(n_r^2+1)^3}\ln\left(\frac{n_r-1}{n_r+1}\right) - 2\frac{n_r^3(n_r^2+2n_r-1)}{(n_r^2+1)(n_r^4-1)} + 8\frac{n_r^4(n_r^4+1)}{(n_r^2+1)(n_r^4-1)^2}\ln(n_r)$$

For any other situation with $0 < n < \infty$, the integral (Eq. 25) must be solved numerically.

As a case study, we can invoke here the calculation of the reflectivity for an air-glass interface, assuming a relative refractive index of 1.55 for glass. In this case, the analytical relation for a collimated radiation field ($n = \infty$) gives $\rho = 0.046$ and the analytical relation for a Lambertian radiation field ($n = 0$) leads to $\rho = 0.099$. This demonstrates that the proposed correction in this case for the incident PFD may vary from 5 to 10% and is not always negligible. The behaviour of this same reflectivity with the degree of collimation *n* may be observed on Figure 6 that displays values given by Eqs. (24-25). One can observe that the quasi-collimated hypothesis for reflectivity calculation (the limit dotted line on Figure 6) is accurate for *n* higher than 20 (with less than 1% deviation).

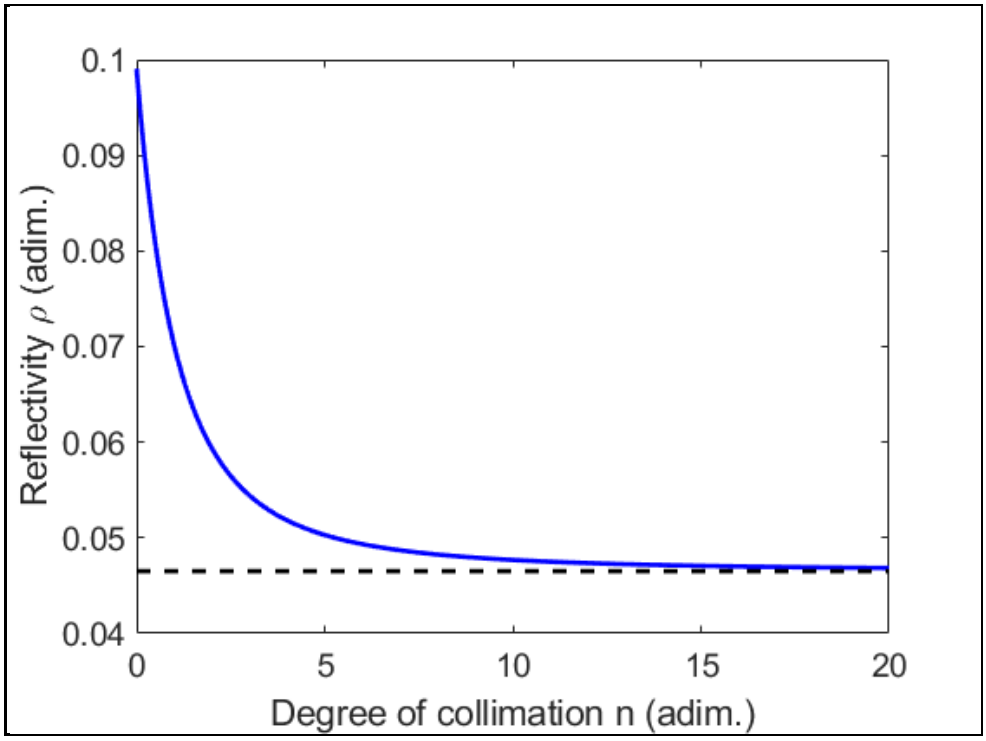


Figure 6: reflectivity of an air-glass interface (n_r = 1.55) as a function of the degree of collimation n (Eq. 25) for the radiation field. One can observe that the two analytical limiting cases for Lambertian radiation (n = 0; ρ = 0.099) and collimated radiation ($n = \infty$; ρ = 0.046) are perfectly given by the general Eq. (25).

RESULTS AND DISCUSSION

In this section, we present and discuss all the experimental results obtained for the two technical setups studied: i) a first setup with constant radial distance for the sources (radius R_C) but varying the radius R_S of the spherical sensor, and ii) a second setup with a unique sensor radius but varying the distance for the sources. For each situation, the light source also is different and representative of the diversity of experimental illuminating systems with degree of collimation varying between n = 13 to 31. For each illuminating system, the value of the mean incident PFD q_R on the fixed P(B)R surface is of course independent of the fluence rate sensor

size and the diameter of the illuminating device. Therefore, we expect to obtain the same q_R value for each of our case study. Indeed, modifications of sensor size R_S or illuminating device radius R_C in Eq. (18) is compensated by the corresponding modification of the view factor $F_{C\to S}$. Thus, obtaining a constant value of the PFD q_R for any of the following experimental situation guarantees first that the view factor $F_{C\to S}$ is properly determined and second that the theoretical relation between fluence rate and incident PFD is correct. It is particularly important to mention at this stage that except from edge effects, it is possible, for each experimental device, to move the fluence rate sensor vertically upwards or downwards at the position *R (or x)* = 0 (center of the photo(bio)reactor, see Figure 5) during a measurement. In this case, a remarkable stability of the signal is observed, even for sources having high degrees of collimation with a great heterogeneity of the sources on the emission surface. This result shows that the proposed method has a strong ability to average these source heterogeneities and at the same time, it ensures a very high accuracy for the average value of the PFD thus determined (estimated experimentally at 5%).

<u>First case study with fixed diameter of the illuminating system, halogen lamps BAB 36-38° (*n* = 13) and two sensor diameters</u>

For this first situation depicted in Material & Methods section (see Figure 1), the results of fluence rate measurements with two sensors and the calculation of the incident PFD from Eq. (18) for three values of the view factor $F_{C\to S}$ (Eqs. 20 & 23) are summarized in Table 1. It clearly appears that the collimated or Lambertian classical assumptions for sources with a beam angle of 36-38° are not adapted to the calculation of the view factor $F_{C\to S}$ and then to the incident PFD at

the rear of the PBR wall. Nevertheless, with a general treatment using a degree of collimation *n* = 13 for the calculation of the exact view factor $F_{C\to S}$ gives exactly the same value q_R = 450 $W.m^{-2}$ = 2300 $\mu mol_{h\nu}.m^{-2}.s^{-1}$ with the two sensors of diameters 3 and 0.15 cm respectively.

This emphasizes the importance to have a complete angular model for the incident radiation generated by the sources, with an exact degree of collimation. This is required to properly calculate the view factor $F_{C\to S}$ according to Eq. 20 & 23, and then obtain an accurate (uncertainty 5%) estimation of the mean incident PFD from the fluence rate measurement at a position *R (or x)* = 0 at the center of the photo(bio)reactor (See Figure 5).

Sensor radius R_S (cm)	Mean photon fluence rate ψ measured ($\mu mol_{h\nu}.m^{-2}.s^{-1}$)	Model of emission at sources	View factor $F_{C\to S}$ (dimensionless)	Calculated photon flux density q_R (Eq. 18) (W/m^2)
3	13000 ± 500	collimated	2.14 x 10^{-1} (Eq. 14)	240 ± 15
		n = 13	**1.20 x 10^{-1} (Eq. 20 & 23)**	**450 ± 20**
		Lambertian	4.07 x 10^{-2} (Eq. 8)	1280 ± 60
0.15	14000 ± 600	collimated	1.07 x 10^{-2} (Eq. 14)	13 ± 1
		n = 13	**3.30 x 10^{-4} (Eq. 20 & 23)**	**450 ± 20**
		Lambertian	1.02 x 10^{-4} (Eq. 8)	1390 ± 70

Table 1: Results for the incident hemispherical radiative flux density (or PFD) q_R in the first case study: P(B)R with radius $R_{P(B)R}$ = 8 cm and semi-height H= 14 cm illuminating system composed of halogen lamps (36-38°) at a fixed emission position radius (R_C = 12 cm). Results obtained with 2 different radii of fluence rate sensor R_S. The PFD can be obtained from the radiative flux (last column) with the conversion factor 1 $W.m^{-2}$ = 5.1 $\mu mol_{h\nu}.m^{-2}.s^{-1}$.

Second case study with fixed sensor diameter, three variable diameters for the illuminating system with LEDs and optics at a beam angle of 24° (n = 31)

For this second situation depicted in Material and Methods section (see Figure 3), the results of fluence rate measurements with three different diameters for the illuminating octagonal system and the calculation of the incident PFD from Eq. (18) for three values of the view factor $F_{C\rightarrow S}$ (Eq. 20 & 23) are summarized in Table 2. Once again, it clearly appears that the collimated or Lambertian classical assumptions for sources with a beam angle of 24° are not adapted to the calculation of the view factor $F_{C\rightarrow S}$ and then to the incident PFD at the wall. Nevertheless, with a general treatment using a degree of collimation n = 31 and calculating the exact view factor (Eq. 20 & 23) gives exactly the same value q_R = 360 W/m^2 = 1660 μmol$_{hν}$.m^{-2}.s^{-1} for the three distances of the sources (R_C of 9.2 cm, 13.9 cm and 18.9 cm respectively) as it should be.

Finally, because all the measurements have been performed in air with the presence of the photo(bio)reactor between the sensor and the sources (two air-glass interfaces), the q_R values obtained in Tables 1 and 2 must be corrected by dividing them by (1 – ρ), with ρ = 0.047 for n = 13 (first case study) and ρ = 0.046 for n = 31 (second case study). This leads respectively to q_R = 470 ± 20 W/m^2 or 2400 ± 100 μmol$_{hν}$.m^{-2}.s^{-1} for the first case and q_R = 380 ± 20 W/m^2 or 1750 ± 90 μmol$_{hν}$.m^{-2}.s^{-1} for the second case.

Radius for the octogonal lighting structure R_C (cm)	Mean photon fluence rate ψ measured ($\mu mol_{h\nu}.m^{-2}.s^{-1}$)	Model of emission at sources	View factor $F_{C\rightarrow S}$ (dimensionless)	Calculated photon flux density q_R (Eq. 18) (W/m^2)
9.2	13800 ± 500	collimated	4.00×10^{-2} (Eq. 14)	300 ± 15
		n = 31	**3.35×10^{-2} (Eq. 20 & 23)**	**360 ± 20**
		Lambertian	1.29×10^{-2} (Eq. 8)	930 ± 40
13.9	10700 ± 400	collimated	4.00×10^{-2} (Eq. 14)	230 ± 10
		n = 31	**2.64×10^{-2} (Eq. 20 & 23)**	**360 ± 20**
		Lambertian	8.49×10^{-3} (Eq. 8)	1100 ± 50
18.9	8500 ±300	collimated	4.00×10^{-2} (Eq. 14)	180 ± 10
		n = 31	**2.10×10^{-2} (Eq. 20 & 23)**	**360 ± 20**
		Lambertian	6.15×10^{-3} (Eq.8)	1200 ± 60

Table 2: Results for the incident hemispherical radiative flux density (or PFD) q_R in the second case study: P(B)R with radius $R_{P(B)R}$ = 7.5 cm and semi-height H=75 cm illuminating system composed of white LEDs (24°) with fixed fluence rate sensor radius (R_S =3 cm). Results obtained for 3 different positions of the sources at distance R_C. The PFD can be obtained from the radiative flux (last column) with the conversion factor 1 $W.m^{-2}$ = 4.6 $\mu mol_{h\nu}.m^{-2}.s^{-1}$.

CONCLUSIONS

In this paper, we rigorously established a theoretical relationship between fluence rate measurement using a spherical sensor placed at the center of a cylindrical illumination device and the average incident photon flux density emitted by the sources (PFD). This theoretical approach not only makes it possible to deal with the classic cases of a collimated or Lambertian incident radiation field, but above all, it is valid for any kind of source as soon as its degree of collimation *n* (properly defined and introduced in the paper from the manufacturers' data) is known. It is then possible to numerically calculate the view factor $F_{C\to S}$ in all generality as established in the article, for example using the web application or the Python code provided along with this article (http://gspr.ip.uca.fr/fluence_rate_view_factor). Knowing this view factor is the preliminary step to calculate the incident PFD in all situations, from a simple measurement of the fluence rate using a spherical sensor put at the centre of the cylindrical device. The approach was then validated on two experimental devices by a redundant approach. In the first case, the diameter of the illuminating system is fixed (constant R_C), but the diameter of the fluence rate sensors varies (variable R_S); in the second case, it is the diameter of the sensor which is fixed (constant R_S) and the diameter of the illuminating system which varies (variable R_C). In all the tested situations, whatever the degree of collimation, the method proved to be very accurate both for the stability of the measurement of the fluence rate (which makes it possible to average the heterogeneities of the emitting wall in a remarkable way) and for the theoretical relations established in this article.

Thus, the method proposed here in the case of radially illuminated photo(bio)reactors proves to be extremely reliable and very simple to implement for accurately calibrating the mean incident

photon flux density, which is an experimental characteristic essential to the description of the kinetic and thermodynamic performances of these photo(bio)reactors. In this case, it appears to be simpler, faster and more accurate than actinometry, which remains the reference method in complex geometry [14]. Additionally, this article clarifies and extends the domain of validity of the relations of the literature for the calculation of reflectivities of the interfaces to the general case of a source with any degree of collimation. This is indeed an important correction step to increase the accuracy in the incident PFD determination.

ACKNOWLEDGMENT

This work was sponsored by a public grant operated by the French National Agency as part of the "Investissements d'Avenir" through the IMobS^3 Laboratory of Excellence (ANR-10-LABX-0016) and the IDEX-ISITE initiative CAP 20-25 (ANR-16-IDEX-0001).

The MELiSSA Pilot Plant is funded from ESA contributions from Spain (main contributor), Begium, France, Italy and Norway, under Frame Contract C4000109802/13/NL/CP. Co-funding from Ministerio de Ciencia e Innovacion (RD 788/2020), Generalitat de Catalunya and Universitat Autonoma de Barcelona is also acknowledged.

ABBREVIATIONS

PFD, mean hemispherical incident photon flux density; P(B)R photo(bio)reactor.

NOMENCLATURE

A_C	Total surface of the surrounding cylindrical illuminating device [m^2]
A_S	Surface of the fluence rate spherical sensor [m^2]
$F_{C\rightarrow S}$	View factor from the surrounding cylinder towards the sensor [adim.]
$F_{S\rightarrow C}$	View factor from the sensor towards the surrounding cylinder [adim.]
G	Spherical irradiance [$\mu mol_{h\nu}.m^{-2}.s^{-1}$ in photonic units or $W.m^{-2}$ in radiant units]

H	Half-height of the illuminating device and/or the photo(bio)eactor [m]
L	Luminance or Specific Intensity [$\mu mol_{hv}.m^{-2}.s^{-1}.sr^{-1}$ for photonic units or $W.m^{-2}.sr^{-1}$ for radiant units]
n	Degree of collimation [0]
n_r	Relative refractive index [adim.]
Q_C	Radiative flux at the surrounding cylinder [$\mu mol_{hv}.s^{-1}$ in photonic units or W in radiant units]
Q_S	Radiative flux at the fluence rate sensor [$\mu mol_{hv}.s^{-1}$ in photonic units or W in radiant units]
q_0	Hemispherical incident light flux density at the surrounding cylinder (light source) [$\mu mol_{hv}.m^{-2}.s^{-1}$ in photonic units or $W.m^{-2}$ in radiant units]
q_R	Hemispherical incident light flux density at the photoreactor wall [$\mu mol_{hv}.m^{-2}.s^{-1}$ in photonic units or $W.m^{-2}$ in radiant units]
R_C	Radius of the surrounding cylindrical illuminating device [m]
$R_{P(B)R}$	Radius of the cylindrical photo(bio)reactor [m]
R_S	Radius of fluence rate sensor [m]
R	Radius [m]
$\vec{r}$	Any space location [m]

x	Abscissa [m]
y	Ordinate [m]

Greek Letters

θ	Polar angle [rd]
θ_B	Beam angle [rd]
θ_V	Viewing angle [rd]
ρ	Reflectivity [adim]
ϕ	Azimuthal angle [rd]
ψ	Fluence rate [$\mu mol_{h\nu}.m^{-2}.s^{-1}$ in photonic units or $W.m^{-2}$ in radiant units]
$\vec{\omega}$	Unit direction for solid angle [sr]
$\vec{\Omega}$	Unit direction for solid angle [sr]

Indices

0	Relative to incident boundary surface
$\perp$	Relative to perpendicular wave
$\parallel$	Relative to parallel wave

REFERENCES

[1] Borowitzka M. A. high-value products from microalgae – their development and commercialization. *J. Appl. Phycol*. **2013**, 25, 743-756.

[2] Serrano B.; De Lasa H. Photocatalytic degradation of water organic pollutants. Kinetic and energy efficiency. *Ind. Eng. Chem. Res*. **1997**, 36, 4705-4711.

[3] Kabra K.; Chaudhary R.; Sawhney R. L. Treatment of hazardous organic and inorganic compounds through aqueous phase photocatalysis: a review. *Ind. Eng. Chem. Res.* **2004**, 43, 7683-7696.

[4] Janin T.; Goetz V.; Brosillon S.; Plantard G. Solar photocatalytic mineralization of 2,4-dichlorophenol and mixtures of pesticides: kinetic model of mineralization. *Solar energy*, **2013**, 87, 127-135.

[5] Wang W.; Ku Y. Photocatalytic degradation of gaseous benzene in air streams by using an optical fiber photoreactor. *J. Photochem. Photobiol A*, **2003**, 159, 47-59.

[6] Da Costa Filho B. M.; Vilar V. J. P. Strategies for the intensification of photocatalytic oxidation processes towards air stream decontamination: a review. *Chem. Eng. Journal*, **2020**, 391, 123531.

[7] Xing Z.; Zong X; Pan J.; Wang L. On the engineering part of solar hydrogen production from water splitting: photoreactor design. *Chem Eng. Sci*. **2013**, 104, 125-146.

[8] Nguyen V-H.; Wu J. C. S. Recent developments in the design of photoreactors for solar energy conversion from water splitting and CO_2 reduction. *Applied Catalysis A*, **2018**, 550, 122-141.

[9] Braun A. M.; Maurette M.T.; Oliveros E. *Photochemical technology*. John Wiley & Sons Ltd, Chichester, **1991**.

[10] Braham R. J.; Harris A. T. Review of major design and scale-up considerations for solar photocatalytic reactors. *Ind. Eng. Chem. Res*. **2009**, 48, 8890-8905.

[11] Legrand J.; Artu A.; Pruvost J. A review on photobioreactor design and modelling for microalgae production. *Reac. Chem. Eng.* **2021**, 299.

[12] Dauchet J.; Cornet J.-F.; Gros F.; Roudet M.; Dussap C.-G. Photobioreactor modeling and radiative transfer analysis for engineering purposes. *Adv. Chem. Eng*. **2016**, 48, chap.1, 1-106.

[13] Cassano A. E.; Martin C. A.; Brandi R. J.; Alfano O. M. Photoreactor analysis and design: fundamentals and applications. *Ind. Eng. Chem. Res*. **1995**, 34, 2155-2201.

[14] Rochatte V.; Dahi G.; Eskandari A.; Dauchet J.; Gros F.; Roudet M.; Cornet J.-F. Radiative transfer approach using Monte Carlo method for actinometry in complex geometry and its application to Reinecke salt photodissociation within innovative pilot-scale photo(bio)reactors. *Chem. Eng. Journal*, **2017**, 308, 940-953.

[15] Dahi G.; Eskandari A.; Dauchet J.; Gros F.; Roudet M.; Cornet J.-F. A novel experimental bench dedicated to the accurate radiative analysis of photoreactors: the case study of CdS catalyzed hydrogen production from sacrificial donors. *Chem. Eng. Process.* **2015**, 98, 174-186.

[16] Zalazar C. S.; Labas M. D.; Martín C. A.; Brandi R. J.; Alfano O. M.; Cassano A. E. The extended use of actinometry in the interpretation of photochemical reaction engineering data. *Chem. Eng. J.* **2005**, 109, 67–81

[17] Roibu A.; Fransen S.; Leblebici M. E.; Meir G.; Van Gerven T.; Kuhn S. An accessible visible-light actinometer for the determination of photon flux and optical pathlength in flow photo microreactors. *Scientific Reports*, **2018**, 8, 5241.

[18] Cornet J.-F. *Procédés limités par le transfert de rayonnement en milieu hétérogène* (in french). Habilitation à Diriger les Recherches (HDR) n° 236, Université Blaise Pascal, Clermont-Ferrand, France, **2007**, p. 249-250. Available from: https://hal.archives-ouvertes.fr/tel-01281239

[19] Mc Naught A. D.; Wilkinson A. *Compendium of Chemical Terminology, "The Gold Book"*, second edition, Blackwell Scientific Publications, Oxford, **1997**.

[20] Siegel R.; Howell J. R. *Thermal Radiation Heat Transfer*, 4th ed.; Taylor and Francis, New York, London, **2002**.

[21] Feingold A.; Gupta K. G. New analytical approach to the evaluation of configuration factors in radiation from spheres and infinitely long cylinders. *Journal of heat transfer, Transactions of the ASME*. **February 1970**, 69-76.

[22] Wu F.-T.; Huang Q.-L. A precise model of LED lighting and its application in uniform illumination system. *Optoelectronics Letters*, **2011**, 7, 1-3.

[23] Moreno I.; Sun C.-C. Modeling the radiation pattern of LEDs. *Optics Express*, **2008**, 16, 1808-1819.

SUPPORTING INFORMATION

Algorithm and Python code for the Monte Carlo assessment of the view factor $F_{C\to S}$ in the general case with any degree of collimation *n* for incident radiant emission at the boundary.

This section summarizes the way to evaluate the view factor $F_{C\to S}$ from eqs (20):

$$F_{C\to S} = \int_{-H}^{H} \frac{dy}{2H} \int_{0}^{2\pi} \frac{d\phi_0}{2\pi} \int_{0}^{1} d\mu_0 \, \mu_0^{n+1} (n+2) \, \mathcal{H}(\Delta) \qquad (20)$$

and (23) in the paper:

$$\Delta = 4 (y \sin\theta_0 \cos\phi_0 - R_C \cos\theta_0)^2 - 4 (R_C^2 + y^2 - R_S^2) \qquad (23)$$

As explained in the text, the triple integral Eq. (20) can be easily interpreted as an expectation in the statistical point of view and evaluated by a numerical procedure using the Monte Carlo algorithm as follows:

- A position y is uniformly sampled between [-H ; H]
- An angle ϕ_0 is uniformly sampled between 0 and 2π
- A value $\mu_0 = \cos(\theta_0)$ is sampled according to the probability density function $p(\mu) = (n+2)\,\mu^{n+1}$. To do so, we uniformly sample a random number r between 0 and 1. The cumulative density function (CDF) corresponding to $p(\mu)$ is $c(\mu) = \int_0^{\mu} d\mu' p(\mu') = \mu^{n+2}$, thus the value of μ_0 that we retain by inverting the CDF is $\mu_0 = r^{\frac{1}{n+2}}$. The pair (ϕ_0, μ_0) defines a direction in the 3D space.
- To assess whether there is an intersection, we compute the discriminant Δ according to Eq (23):
    - If $\Delta \geq 0$, there exists an intersection and we count $w = 1$
    - If $\Delta < 0$, there is no intersection and we retain $w = 0$

Finally, the above sampling procedure is repeated N times and the view factor is estimated by the average of the N w samples. The 95% confidence interval is provided from the standard deviation of the w set .

A Python code has been developed to implement this algorithm and is also proposed hereafter for the interested reader (the input data correspond here to the first case study of the paper with halogen lamps BAB 36-38° and the collimation factor n = 13):

```python
import numpy as np

Rs = 3
Rc = 12
H = 14
n = 13
n_samples = 100000
np.random.seed(0)
w=0 # Initialisation of the sum of the weight
w2=0 # Initialisation of the sum of the squared weight, to compute the variance

for i in range(0,n_samples):
    ###############################################################################
    ##### Uniform sampling of a location on the cylinder and of an angle phi #####
    ###############################################################################
    y=(1-2*np.random.rand(1))*H
    phi=np.random.rand(1)*2*np.pi

    ###############################################################################
    #####    Sampling of mu=cos_theta according to the PDF 1/(n+2)*mu^(n+1)  #####
    ###############################################################################
    mu=np.random.rand(1)**(1/(n+2))
    cos_theta=mu

    ###############################################################################
    #####       Definition of sin_theta using cos_theta^2+sin_theta^2=1      #####
    ###############################################################################
    sin_theta=np.sqrt(1-cos_theta**2);

    ###############################################################################
    #####  Test if there is an intersection between the ray and the sphere   #####
    ###############################################################################

    delta=(2*(y*sin_theta*np.cos(phi)-Rc*cos_theta))**2-4*(Rc**2+y**2-Rs**2);

    ###############################################################################
    #####          In case of an intersection, update of the weights         #####
    ###############################################################################
    if delta>=0:
        w+=1
        w2+=1

###############################################################################
#####       Computation of the view factor VF and its uncertainty        #####
###############################################################################

VF=w/n_samples
uncertainty=2*((w2/n_samples-VF**2)/(n_samples-1))**(1/2)

entry=f'{VF:.4e}'+u'\u00B1'+f'{uncertainty:.4e}'

print(entry)
```

Except for the inputs/outputs, this Python code is exactly the code executed when using the web interface for the $F_{C\rightarrow S}$ view factor calculation at

http://gspr.ip.uca.fr/fluence_rate_view_factor.